# Autoperfused mouse flow chamber reveals synergistic neutrophil accumulation through P-selectin and E-selectin

Michael L. Smith,* Markus Sperandio,*,†,[1] Elena V. Galkina,‡ and Klaus Ley*,‡

*Department of Biomedical Engineering and ‡Cardiovascular Research Center, University of Virginia, Charlottesville; and †Neonatal Unit, Children's Hospital, University of Heidelberg, Germany

**Abstract: To study rolling of mouse neutrophils on P- and E-selectins in whole blood and without cell isolation, we constructed an autoperfused flow chamber made from rectangular microslides (0.2×2 mm) perfused from a carotid artery catheter. A differential pressure transducer served to measure wall shear stress. Green fluorescent neutrophils rolled on P-selectin but not E-selectin coated at 50 ng/ml, with some rolling on E-selectin at 150 ng/ml. However, when P- and E-selectins were coimmobilized, the resulting number of rolling neutrophils was sixfold and fourfold higher than on P- or E-selectin alone. Velocity and flux analysis shows that P-selectin initiates neutrophil rolling, and a small amount of E-selectin, unable to capture many neutrophils, reduces the rolling velocity of all neutrophils by more than 90%. The unexpected synergism between E- and P-selectins explains why neutrophil recruitment is enhanced when both selectins are expressed. *J. Leukoc. Biol.* 76: 985–993; 2004.**

***Key Words:*** *leukocyte rolling · capture · shear stress*

## INTRODUCTION

Leukocyte recruitment begins through adhesive interactions between leukocytes and the endothelium, which mediate the capture of free-flowing leukocytes from the blood, leukocyte rolling along the endothelium, and firm arrest on and transmigration through the endothelium [1].

Although intravital microscopy is a powerful tool for the study of leukocyte rolling in vivo, the rolling environment in venules is complex. Wall shear stress in venules varies with volume flow rate, tube hematocrit, and diameter and changes along the venular tree, as vessel diameter and volume flow rate change. In addition, the endothelium is lined with an endothelial surface layer, and there is increasing evidence that this layer retards the flow of plasma [2] and limits the accessibility of adhesion molecules [3]. Numerous adhesion molecules are expressed on the endothelium at variable site densities along the length of the vessel and alter rolling velocity or adhesion dynamics locally [4, 5].

As a result of the complexity of leukocyte rolling on native endothelium in vivo, flow chamber systems have been particularly useful in the elucidation of numerous aspects of leukocyte rolling and adhesion, including the need for selectins in the capture of neutrophils from free flow and the subsequent requirement for integrins in firm adhesion of neutrophils [6], the ability of $\alpha_4$ integrins to initiate lymphocyte tethering and rolling in the absence of selectins [7], the shear threshold for selectin-mediated rolling [8, 9], and the role of chemokines in leukocyte arrest [10, 11].

Parallel plate-flow chambers were used as early as 1912 for numerous tissue-culture applications [12, 13]. Since the flow chamber was first used to study selectin- and integrin-mediated leukocyte rolling and adhesion in 1987 [14], numerous design modifications have been described. These modifications include a chamber with a linear variation in shear stress from the entrance to the exit [15], a chamber perfused with pulsatile flow [16], a side-view flow chamber [17], and a cylindrical flow chamber, allowing lateral visualization of leukocytes flowing in whole blood [18]. A novel flow chamber was also described that allowed visualization of platelet deposition ex vivo; the flow chamber was coupled directly to the carotid artery of a heparinized pig [19]. A flow chamber perfused with whole blood [20] or coupled to an animal ex vivo [19] would not require leukocyte subset isolation. Isolation procedures are known to activate neutrophils, resulting in increased expression of Mac-1 integrin and decreased expression of L-selectin [21–23].

Despite the important contributions flow chambers have made to the field of leukocyte rolling and adhesion, current limitations include the large dead volume of fluid, ~1500 μl, and the high cell cost necessary to perform an experiment. A popular, commercially available system (GlycoTech, Rockville, MD) reduced the dead volume to ~225 μl [24], but the requirement to isolate large numbers of cells still limits the use of flow chambers for rare leukocyte populations such as eosinophils or isolated leukocytes from species such as the mouse. A recently published negative immunomagnetic isolation protocol yields $\sim 0.5 \times 10^6$ neutrophils/ml whole mouse blood [25]. For an experiment requiring $1 \times 10^6$ isolated neutrophils/ml perfusion media and a best-case yield of 1.5 ml whole blood/mouse, perfusion at 1.0 ml/min (~0.5 dyn/cm$^2$) for 10 min through a GlycoTech flow chamber would require the

[1] Correspondence: Universität Heidelberg, Children's Hospital, Im Neuenheimer Feld 150, 69120 Heidelberg, Germany. E-mail: markus_sperandio@med.uni-heidelberg.de

Received October 16, 2003; revised February 20, 2004; accepted February 23, 2004; doi: 10.1189/jlb.1003483.

sacrifice of at least six mice, which probably explains the absence of flow-chamber studies conducted with mouse leukocytes. Gene-targeted deletion of adhesion molecules offers ideal conditions to study adhesive interactions between distinct pairs/groups of adhesion molecules. In addition, transgenic mice have been generated, which express enhanced green fluorescent protein (GFP) in neutrophils using the endogenous lysozyme M promoter [26], allowing visualization of neutrophils by epifluorescence microscopy.

To extend the application of flow-chamber technology to the mouse, we developed a microflow-chamber system with an autoperfused, extracorporal, arteriovenous circuit and used it to investigate possible synergistic effects between P- and E-selectin. A commercially available chamber was chosen based on its low cost and history of leukocyte rolling studies [20]. P-selectin is expressed in endothelial cells and platelets, rapidly up-regulated, and binds to P-selectin glycoprotein ligand-1 (PSGL-1). E-selectin is expressed by endothelial cells and binds to PSGL-1 and other ligands. E-selectin is not efficient at capturing cells from free flow [27, 28] but mediates slow leukocyte rolling in vivo [29]. It is interesting that there is no evidence for a major difference in molecular off-rate between P- and E-selectins [30]. It is known that P- and E-selectins must be blocked to profoundly reduce neutrophil recruitment [31, 32], suggesting overlapping functions. Possible synergistic functions of E- and P-selectins have not been investigated so far, but the strikingly different phenotype of E- versus P-selectin versus E/P double-knockout mice suggests that such interactions may exist.

Here, we use a novel, autoperfused flow chamber to test the hypothesis that efficient neutrophil capture by P-selectin and slow rolling through E-selectin synergize to enhance the accumulation of rolling neutrophils observed on either selectin alone.

## MATERIALS AND METHODS

### Animals

C57Bl/6 mice and transgenic mice, in which the enhanced GFP gene was knocked into the murine lysozyme M (lys) locus [26], back-crossed to Bl/6 for at least 10 generations (kind gift of Dr. Thomas H. Graf, Albert Einstein College of Medicine, Bronx, NY), were housed in a barrier facility under specific, pathogen-free conditions. The Animal Care and Use Committee of the University of Virginia (Charlottesville) approved all animal experiments. Mice were anesthetized and placed on a 38ºC heating pad [2]. The trachea was intubated using polyethylene (PE)90 tubing [inner diameter (ID), 0.86 mm; outer diameter (OD), 1.27 mm; Becton Dickinson, San Jose, CA]. The left jugular vein and left carotid artery were cannulated using PE10 (ID, 0.28 mm; OD, 0.61 mm) or PE50 tubing (ID, 0.58 mm; OD, 0.965 mm), depending on the wall shear-stress regime desired in the flow chamber (see below). For carotid artery cannulation with PE50 tubing, the cannula had to be drawn to reduce the diameter at the tip. This was limited to a short section (typically, <0.5 cm) to limit pressure drop in the tubing.

### Recombinant proteins and antibodies

Recombinant murine P- and E-selectin/Fc (150 ng/ml, R&D Systems, Minneapolis, MN) bind leukocytes under static and dynamic conditions [33]. Blocking monoclonal antibody (mAb) RB40.34 [rat immunoglobulin G1 (IgG1), 30 μg/mouse; ref. 34] against P-selectin was kindly provided by Dr. Dietmar Vestweber (University of Münster, Germany). E-selectin-blocking mAb 9A9 (rat IgG1, 30 μg/mouse; ref. [35]) blocks E-selectin-dependent rolling in vivo and in vitro and was kindly provided by Dr. Barry Wolitzky (MitoKor, San Diego, CA).

### Flow cytometry

Heparinized blood was collected from individual mice for determination of GFP expression on different subsets. Red blood cells were lysed using 0.834% $NH_4Cl$, and white blood cells (WBC) were washed twice with calcium- and magnesium-free phosphate-buffered saline (PBS) and incubated with mAb RB66-8C5–allophycocyanin (APC) (Gr-1), M1/70–phycoerythrin (PE; CD11b), and rat $IgG_{2b}$–APC and –PE (BD Biosciences, San Diego, CA) for 20 min at 4°C in staining buffer (0.3% bovine serum albumin, 0.2% $NaN_3$ in PBS–CMF), washed twice, resuspended in staining buffer containing 2% formaldehyde, and analyzed the following day. Flow cytometry was performed on a FACSCalibur (Becton Dickinson) and analyzed using WinMDI software (Joseph Trotter, Scripps Institute, La Jolla, CA). Peripheral blood neutrophils were characterized by forward-scatter, side-scatter, and expression of GR-$1^{high}$/CD11$b^{inter}$ [36]. Most neutrophils in blood were GFP-positive (95%±1%, n=6) and expressed very high GFP levels (data not shown). Most monocytes (Gr$1^{inter}$/CD11$b^{high}$) expressed GFP at low levels (data not shown). GFP expression was found on a small fraction of Gr-$1^-$ cells as well, consistent with a previous report [26].

### Chamber assembly

Rectangular glass capillaries (0.2×2 mm, VitroCom, Mountain Lakes, NJ) were cut into chambers of various lengths using a capillary cutting stone (Hampton Research, Aliso Viejo, CA). Flow chambers were first connected to a 1-cm piece of silastic tubing (ID, 1.45 mm; OD, 1.96 mm; Dow Corning, Midland, MI) into which two PE50 tubes or one PE50 tube and one PE100 tube (ID, 0.86 mm; OD, 1.52 mm) of lengths 5 and 20 cm, respectively, were inserted. These two tubing combinations were chosen to produce low (two PE50 tubes) or high (one PE50 and one PE100) wall shear-stress regimes. For ex vivo microscopy experiments, recombinant murine P- and/or E-selectin/Fc (R&D Systems) were introduced into the chamber's free end via capillary action. The free end was then inserted into a second piece of silastic tubing into which two PE50 tubes or one PE50 tube and one PE100 tube were inserted, and all joints were sealed with two-part epoxy resin (Loctite, Manco Inc., Avon, OH). Adhesion molecules were coated for 2 h at room temperature, followed by Tween 20 (0.5% in PBS) for 1 h at room temperature to block nonspecific adhesion [37].

### Pressure-transducer calibration

For differential pressure-transducer calibration, a wet/wet low differential pressure transmitter model PX154-003DI (Omega Engineering, Stamford, CT), with the analog output in milliamperes (mA) read on a model DP24-E economical process meter (Omega Engineering), was connected to a water manometer with the low-pressure end open to the atmosphere. Large-diameter, clear, polyvinyl-chloride tubing (ID, 6.35 mm; OD, 7.94 mm; Fisher Scientific, Pittsburgh, PA), which limits hysteresis, was connected to an air-filled syringe with a three-way stopcock (Medex, Hilliard, OH) used to incrementally manipulate pressure head across the transducer. To determine pressure drop during whole mouse blood perfusion, the flow chamber was perfused with heparinized (10 U/ml) whole mouse blood obtained via heart puncture (n=4 mice; hematocrit, 34–40%) using a syringe pump (model 22, Harvard Apparatus, Holliston, MA) at defined volume flow rates. For plasma perfusion, whole mouse blood was centrifuged at 600 *g* for 10 min, and the plasma was transferred to a fresh tube. Plasma viscosity was measured at room temperature using a Cannon-Manning semi-micro viscometer (Cannon Instrument Co., State College, PA), and blood hematocrit was measured using a Hemavet 850 (CDC Technologies, Oxford, CT).

### Ex vivo microscopy

Each flow chamber was flushed with heparin in saline (10 U/ml) and rinsed with saline. For low wall shear stress, chambers with two PE50 tubes were connected to PE10 carotid artery and jugular vein cannulas (**Fig. 1A**). Figure 1B shows a photograph of a 20-mm long flow chamber with two PE50 tubes inserted into each end. One PE50 tube on each end is connected in series to a PE10 tube denoted by arrows. For high wall shear stress, PE100 tubes were

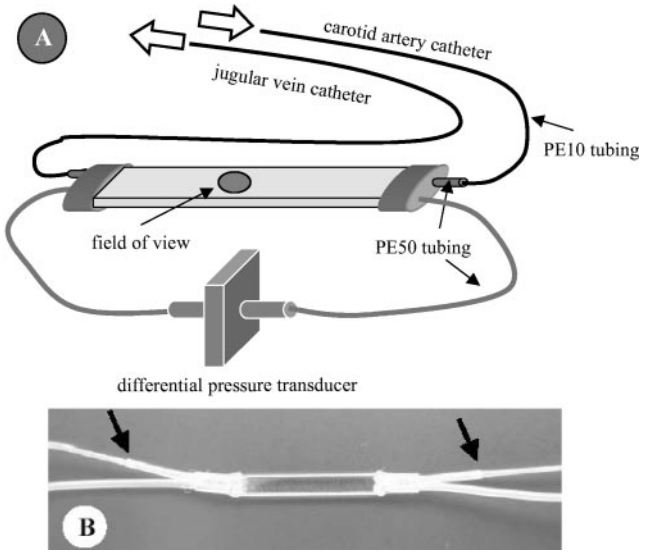


**Fig. 1.** Schematic representation of the microslide flow chamber and accessories, with the upstream end receiving blood from the carotid artery cannula and the downstream end feeding blood into the jugular vein (A). Block arrows denote the direction of blood flow. (B) Photograph shows two PE50 tubes exiting the flow chamber at each end. One PE50 tube at each end of the chamber is connected in series to a PE10 tube, denoted by arrows, without the use of epoxy resin for rapid exchange of the flow chamber.

connected to PE50 carotid artery and jugular vein cannulas. The tight fit of PE10 inside PE50 or PE50 inside PE100 did not require the use of epoxy resin, allowing multiple flow chambers to be used per mouse. The second set of PE50 tubes for either chamber assembly was used for infusion of antibodies and for measurement of pressure drop across the flow chamber. The pressure-transducer-baseline was determined at the beginning and end of each experiment, and the carotid artery cannula was clamped shut, and pressure-drop measurements were not included if the baseline drifted by more than 10% during the course of the 10-min experiment. Differential WBC counts were measured before and after each flow-chamber perfusion period from 30 μl whole blood drawn from the carotid artery cannula using the Hemovet 850.

Microscopic observations were made on a Zeiss intravital microscope (Axioskop, Carl Zeiss, Inc., Thornwood, NY) with a saline immersion objective (SW 20/0.5 or SW 40/0.75) visualized using stroboscopic flash (Strobex 236, Chadwick Helmuth, Mountain View, CA) epi-illumination to limit light-dye damage to the cells. Flow chambers were superfused with 37°C water to limit temperature changes in the extracorporeal circuit. Recordings were made through a charged-coupled device camera (model VE-1000CD, Dage-MTI, Michigan City, IN) on a Panasonic S-VHS recorder. The microscope field of view (FOV) was consistently placed over the central axis of the flow chamber 1 cm downstream from the inlet to limit the impact of leukocyte interaction variability along the length and width of the flow chamber [38].

## Pressure and flow

Mean wall shear stress, $\bar{\tau}_w$, was estimated from the overall pressure drop, $\Delta P$, along the length of a flow channel, $L$, necessary to drive flow an average velocity $\bar{U}$. Wall shear stress is considered a mean value, as it deviates around the wetted perimeter of the channel cross-section, $p$, with a minimum in the channel corners. The relationship between $\Delta P$ and $\bar{\tau}_w$ requires that the entrance length, $L_e$, be much smaller than $L$. The entrance length in laminar flow was estimated using:

$$L_e = 0.05 D_h(\mathrm{Re}_{D_h}), \tag{1}$$

where $D_h$ is the hydraulic diameter, and $\mathrm{Re}_{D_h}$ is the Reynolds number calculated using the hydraulic diameter as the characteristic length [39]. These quantities are calculated using:

$$D_h = \frac{4A}{p} \quad \text{and} \quad \mathrm{Re}_{D_h} = \frac{\bar{U} D_h}{v}, \tag{2}$$

where $A$ is the cross-sectional area of the chamber equal to width, $w$, times height, $h$, and $v$ is kinematic viscosity. Using a control volume analysis of the flow chamber containing fluid with density ρ, rearrangement and integration of a sum of forces on the control volume over the length of the flow chamber yield [40]:

$$\bar{\tau}_w = \frac{\Delta P D_h}{4L}. \tag{3}$$

Equation (3) does not assume that the fluid is Newtonian, but it does invoke the continuum approximation. The continuum approximation is appropriate for physiological hematocrits flowing through glass capillaries as small as 20 μm in diameter [41], well below the hydraulic diameter of 360 μm for the glass capillaries used here. A more detailed analysis was used to determine mean velocity and volume flow rate through the channel, $Q$, to verify that $L_e << L$. The Fanning friction factor, $f$, is customarily defined as the ratio of friction to inertia forces:

$$f = \frac{\bar{\tau}_w}{\tfrac{1}{2}\rho \bar{U}^2}. \tag{4}$$

For a rectangular cross-section with $h/w = 0.1$, $f$ equals $21.17/\mathrm{Re}_{D_h}$. The relationship between volume flow rate and average velocity, $Q = \bar{U}A$, and rearrangement of equations (4) and (5) yield:

$$Q = \left(\frac{\Delta P D_h}{2\rho f L}\right)^{1/2} wh. \tag{5}$$

The Womersley number, $Wo$, was used to determine if unsteady effects, as a result of pulsatility of flow from the carotid artery, limit the use of an average wall shear-stress value in the flow chamber. For pulsating flow in pipes with a frequency of applied pressure gradient $n$, the dimensionless Womersley number is:

$$f = \frac{\bar{\tau}_w}{\tfrac{1}{2}\rho \bar{U}^2}. \tag{6}$$

For $Wo$ values less than unity, flow is quasi-steady, and an average wall shear stress over time is acceptable [42, 43]. Flow is considered quasi-steady if the instantaneous velocity profile corresponds to what would be expected for the instantaneous pressure-gradient driving flow.

## Data analysis

A MicroMotion DC30 video compression card (Pinnacle Systems, Mountain View, CA) was used to digitize video recordings from a JVC HR-53600U VHS recorder into a Macintosh computer (Adobe Premiere software). Digitized video clips were analyzed with the public domain NIH Image program (http://rsb.info.nih.gov/nih-image/). All analysis was performed using custom-written macros similar to ones described previously [44]. Rolling velocities of GFP-expressing neutrophils were calculated by measuring the distance that cells rolled during a 1- or 2-s time interval for cells translating greater than or less than 100 μm/s, respectively. Ten leukocytes were measured per FOV for at least four independent experiments in each group. Rolling flux, $\dot{F}$, was determined from the number of rolling cells per FOV (570×420 μm surface area), $R$, and the harmonic mean of the rolling velocity measurements, $\bar{V}$, according to

$$\dot{F} = \frac{R}{l_{FOV}} * \bar{V}, \tag{7}$$

where $l_{FOV}$ is the width of the FOV (570 μm), assuming the camera is aligned for cells to roll horizontally across the video screen. Data were expressed as mean ± SEM and compared by two-tailed $t$-test with $P = 0.05$.

# RESULTS

## Calibration

To determine wall shear stress in the autoperfused flow chamber, a differential pressure transducer was calibrated using a

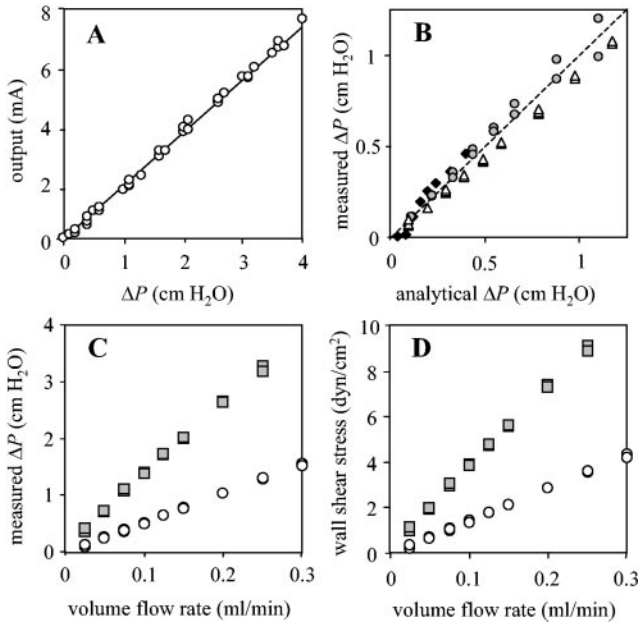


**Fig. 2.** Differential pressure-transducer calibration. Transducer output, in mA, as a function of pressure difference measured by water-filled manometer (n=4 trials; A). Solid line, least-squares linear regression forced through the origin [output (mA)=1.86×pressure drop (cm $H_2O$), $R^2$=0.998]. Comparison of directly measured pressure difference ($\Delta P$; ordinate) and predicted pressure difference, in cm $H_2O$, estimated from a known volume flow rate set on a syringe pump and equation (7) for saline (B). Flow chambers with lengths of 1.3 (◆), 3.2 (△), and 3.6 cm (●) perfused with mouse blood at volume flow rates ranging from 0.025 to 0.5 ml/min (n=2 for each flow chamber). Measured pressure difference (ordinate; C) and wall shear stress (ordinate; D) as a function of volume flow rate for whole mouse blood (■; hematocrit, 34–40%, n=3 animals in three flow chambers) and plasma (○; n=3 flow chambers) for volume flow rates from 0.025 to 0.3 ml/min.

water-filled manometer. Pressure head was manipulated in the manometer using an air-filled syringe and a three-way stopcock through a range of 0–4 cm $H_2O$, and pressure-transducer output, in mA, was plotted as a function of pressure head (**Fig. 2A**). The slope of a line fit to the data and forced through the origin was used in all subsequent experiments to convert pressure-transducer output to pressure drop [output (mA)= 1.86×pressure drop (cm$H_2O$), $R^2$=0.998].

To further validate the calibration curve in the presence of flow, the pressure transducer was used to predict the known volume flow rate of a Newtonian fluid perfused through the flow chamber with a syringe pump. Predicted pressure drop was calculated using the dimensions of the flow chamber and fluid properties of saline using equation (5). Three flow chambers of lengths 1.3, 3.2, and 3.6 cm were perfused with 0.025–0.5 ml/min (n=2 for each flow chamber). Measured pressure drop, using the calibration curve from Figure 2A, is shown versus predicted pressure drop calculated with equation (5) in Figure 2B ($R^2$=0.988). For a given volume flow rate, pressure drop scales linearly with flow chamber length, and hence, chamber length is an important parameter in the determination of wall shear stress through the chamber.

Calibration was extended to pressure drop as a result of perfusion of mouse plasma or whole blood through the flow chamber. Heparinized whole mouse blood with hematocrits from 34 to 40% or mouse plasma was perfused through three different flow chambers at volume flow rates from 0.025 to 0.3 ml/min, and measured pressure drop was plotted versus volume flow rate for one representative flow chamber of length 2.1 cm and hematocrit 40% (Fig. 2C). For a given volume flow rate and flow chamber length, whole mouse blood consistently resulted in an ~2.5-fold increase in pressure drop over mouse plasma. Wall shear stress was computed from the measured pressure drop using equation (3) and plotted versus volume flow rate for one representative flow chamber of length 2.1 cm and hematocrit 40% (Fig. 2D). Wall shear stress is linearly dependent on pressure drop, and whole mouse blood again resulted in an ~2.5-fold increase in wall shear stress over plasma at constant volume flow rate and flow chamber length.

## Ex vivo microscopy

GFP-positive leukocytes were seen moving in close proximity to the upper wall of autoperfused flow chambers without coated adhesion molecules. To assess the impact of pulsatility associated with blood flow in the carotid artery, leukocyte displacements were tracked frame by frame using the low wall shear-stress tubing combination (PE10/50) to determine instantaneous velocities as a function of time and used as an indirect indicator of pulsatility. **Figure 3A** shows tracings of three leukocytes tracked in flow chambers from different mice. From a pool of 10 mice, the two tracked cells with the most extreme pulsatility, the largest difference between the maximum and minimum velocities, are shown (△ and ◆). The third leukocyte shows a typical velocity tracing with a range of 720–880 μm/s. All leukocyte tracings were consistent with a heart rate of ~200 beats/min.

Wall shear stress was calculated in autoperfused flow chambers with low (PE10/50) or high (PE50/100) wall shear-stress tubing combinations using pressure drop and equation (3). Figure 3B shows the mean and SEM for six representative flow chambers in four different mice and six representative flow chambers in five different mice using the low or high wall shear-stress tubing, respectively, during the course of a 10-min

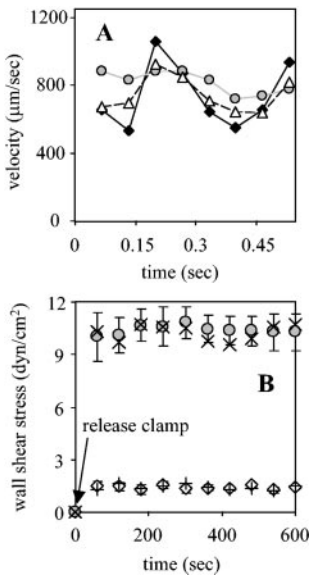


**Fig. 3.** Velocity of GFP-expressing, free-flowing neutrophils near the upper wall of flow chambers perfused from transgenic mice (A). Cells flowing near the upper wall (less than 10 μm) but not interacting with the wall. Representative cells from 10 flow chambers connected with PE10/50 tubing showing average (●) and highest observed pulsatility (◆ and △). (B) Mean ± SEM of wall shear stress from six representative flow chambers from four mice using PE10/50 (◇) or six representative flow chambers from five mice using PE50/100 (●) through the course of a 10-min perfusion period. Representative individual flow chambers shown as + or × for low or high shear-stress tubing combinations, respectively. Release of a clamp to initiate perfusion of the chamber at time = 0.

TABLE 1. Flow Chambers Perfused from Mice

| | | $\Delta P/L$ (cm $H_2O$/cm) | $\bar{\tau}_w$ (dyn/cm$^2$) | $Q$ (ml/min) | $Re_{D_h}$ | $L_e$ (μm) | Wo |
|---|---|---|---|---|---|---|---|
| | Low | 0.07 | 0.6 | 0.02 | 0.12 | 2.6 | 0.53 |
| 10/50 | Mean | 0.16 | 1.4 | 0.047 | 0.28 | 6.1 | 0.53 |
| | High | 0.28 | 2.5 | 0.083 | 0.5 | 11 | 0.53 |
| | Low | 0.81 | 7.3 | 0.24 | 1.46 | 32 | 0.53 |
| 50/100 | Mean | 1.15 | 10.3 | 0.34 | 2.06 | 45 | 0.53 |
| | High | 1.47 | 13.1 | 0.44 | 2.64 | 58 | 0.53 |

Pressure drop per unit length, wall shear stress, volume flow rate, Reynolds number, entrance length, and Womersley number in 0.2 × 2 mm flow chambers perfused from mice through PE10/50 or PE50/100 tubing.

perfusion period. The carotid artery clamp was released at time = 0. Wall shear stress varied little between different flow chambers and in a single flow chamber during the course of perfusion with an average of 1.38 ± 0.16 or 10.4 ± 0.4 dyn/cm$^2$ in low or high wall shear-stress flow chambers. In addition, one representative flow chamber from each wall shear stress regime is plotted in Figure 3B to illustrate the behavior within individual flow chambers during an experiment. Of note, this wall shear stress is determined experimentally without having to make assumptions about blood viscosity.

**Table 1** provides details for pressure drop per unit length of chamber ($\Delta P/L$), $\bar{\tau}_w$, $Q$, $Re_{D_h}$, $L_e$, and Wo for the mean, minimum, and maximum wall shear-stress values from 22 low and eight high wall shear-stress regime flow chambers. An increase in the ID of the carotid artery and jugular vein cannulas from 0.28 to 0.58 mm reduced pressure drop in the tubing and greatly increased pressure drop in the flow chamber. Flow through the chamber was laminar and quasi-steady, as reflected by $Re_{D_h}$, which was less than three, and the Womersley number, which was ~0.5. Based on these measurements, unsteady effects as a result of pulsatility of flow from the carotid artery do not limit the use of an average wall shear-stress value in the flow chamber, and the entrance length only accounts for less than 0.3% of the total length of the flow chamber.

GFP neutrophils in whole blood were tested for their ability to interact specifically with P-selectin/Fc using the PE10/50 tubing combination. Flow chambers were coated with P-selectin/Fc for 2 h at room temperature (150 ng/ml), followed by a 1-h block at room temperature with Tween 20 (0.5% in PBS) and a rinse with heparin in saline (10 U/ml). GFP-positive neutrophils were seen rolling on the upper wall of the flow chamber (**Fig. 4A**). Infusion of anti-mouse P-selectin mAb Rb40.34 but not anti-mouse E-selectin mAb 9A9 through the second upstream PE50 tube completely abrogated this rolling (n=3; Fig. 4B). The mAb infusion rate was set on a syringe pump at 0.01 ml/min, ~25% of the volume flow rate of whole blood through the chamber (see above). No rolling or nonspecific adhesion was seen in flow chambers that were blocked with Tween 20 in the absence of a selectin (Fig. 4C).

To assess the impact of the extracorporeal circuit on systemic leukocyte counts, three flow chambers were autoperfused for 10 min each (total of 30 min autoperfusion) in four mice, and blood samples were taken before and after each perfusion period for the analysis of peripheral neutrophil and monocyte counts. **Figure 5** illustrates that neither neutrophil nor monocyte counts changed after each of three consecutive flow chambers from the control sample taken before autoperfusion. Neutrophil and monocyte counts averaged 312 ± 20 cells/μl and 182 ± 19 cells/μl in whole blood, respectively.

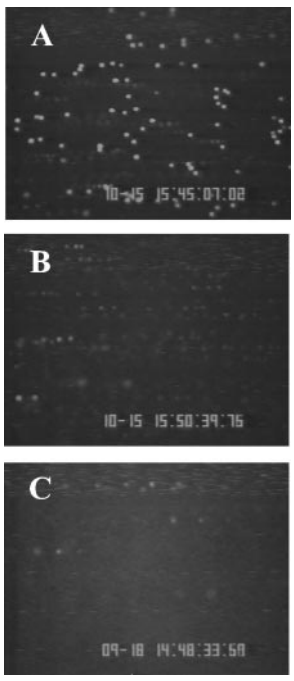


**Fig. 4.** Photomicrographs showing flow chambers perfused from Lys–GFP-transgenic mice coated with recombinant mouse P-selectin/Fc (150 ng/ml) and blocked with Tween 20 before (A) and after infusion of anti-mouse P-selectin mAb RB40 (B). Flow chamber with no P-selectin and blocked with Tween 20 only (C). FOV height and width, 420 × 570 μm. Note that stroboscopic epi-illumination produces multiple images of the same cell in a field, creating the appearance of strings, but this is an imaging artifact and not related to strings caused by secondary capture [45, 46]. Flow from left to right.

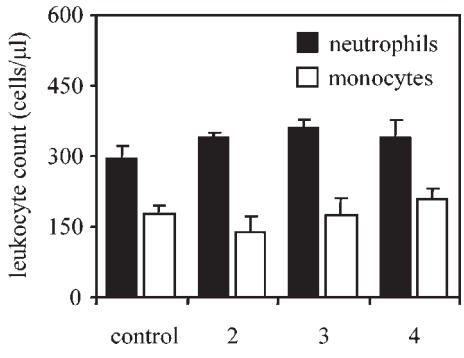


**Fig. 5.** Systemic neutrophil (solid bars) and monocyte (open bars) counts shown as mean ± SEM for four mice before and after autoperfusion of each of three flow chambers (1–3) per mouse. An automatic blood cell counter measured samples (30 μl) drawn from carotid artery cannula.

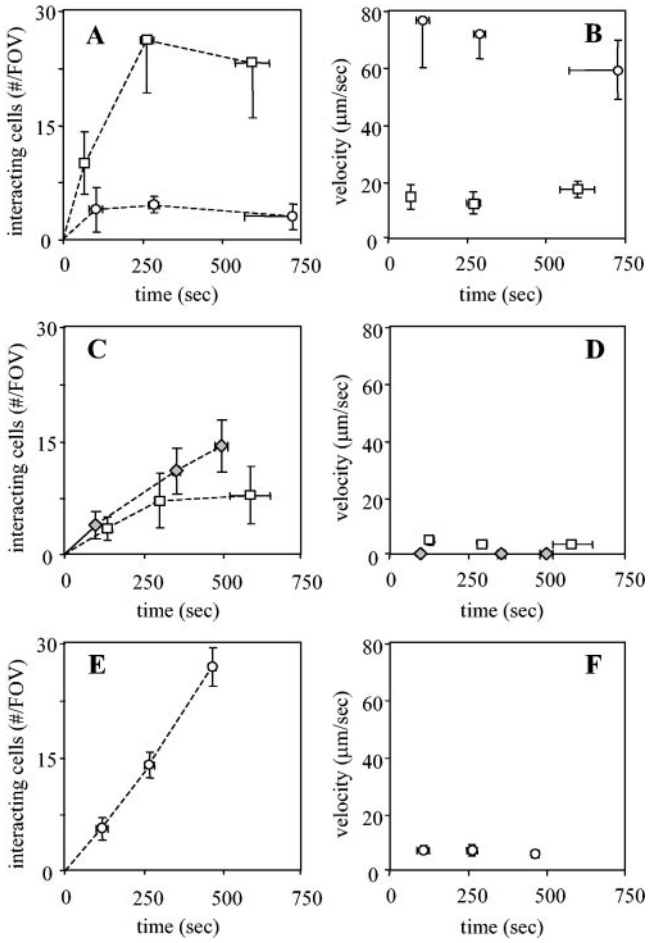


**Fig. 6.** Numbers (A) and velocities (B) of rolling GFP neutrophils per FOV (570×420 μm) on P-selectin coated at 50 ng/ml (○) or 150 ng/ml (□). Numbers (C) and velocities (D) of rolling GFP neutrophils per FOV on intermediate (150 ng/ml, □) or high (600 ng/ml, ◇)-coating concentrations of mouse E-selectin/Fc. Numbers (E) and velocities (F) of GFP neutrophils per FOV on coimmobilized mouse E-selectin/Fc (150 ng/ml) and P-selectin/Fc (50 ng/ml). Each data point is mean ± SEM for at least four flow chambers from at least three different mice.

GFP-neutrophil rolling interactions were quantified on mouse P-selectin/Fc or E-selectin/Fc at low (50 ng/ml coating concentration), intermediate (150 ng/ml), and high (600 ng/ml) site densities at multiple time-points after the initiation of autoperfusion. These experiments were performed using the low wall shear-stress tubing combination with flow chambers between 2 and 3 cm in length. Mean wall shear stress for all 22 flow chambers used to acquire data for **Figure 6** was 1.41 ± 0.03 dyn/cm$^2$, resulting in a mean pressure drop of 0.36 ± 0.015 cm $H_2O$. GFP neutrophils accumulated in a time-dependent manner on P-selectin/Fc with an increase in the number of rolling cells per FOV (Fig. 6A) and a decrease in rolling velocity with increasing coating concentration (Fig. 6B). GFP neutrophils did not interact with low-density E-selectin/Fc, but cells interacted (Fig. 6C) and rolled at a consistently low-rolling velocity (4.0±1 μm/s; Fig. 6D) on the intermediate coating concentration. On the high coating concentration, cells became firmly adherent directly without rolling (Fig. 6, C and D). This appeared to be only a selectin site-density effect, however, as the cells did not spread and assume a "fried-egg" pattern as was seen for adherent cells on coimmobilized P-selectin, intercellular adhesion molecule-1 (ICAM-1), and interleukin-8 [37]. Despite a fourfold increase in E-selectin-coating concentration, GFP-neutrophil accumulation was only slightly increased above intermediate E-selectin, and this increase was only statistically significant at the latest time-point (Fig. 6C).

To test the hypothesis that P-selectin serves as a tethering molecule for neutrophils allowing slow rolling mediated through E-selectin, GFP-neutrophil interactions were quantified on coimmobilized, low-coating concentration P-selectin/Fc and intermediate-coating concentration E-selectin/Fc. Although low-density P-selectin/Fc only supported 2.7 ± 1.7 rolling cells per FOV, and intermediate-density E-selectin/Fc supported 7.8 ± 3.8 rolling cells per FOV at the latest time point, the coimmobilization of both selectins greatly enhanced tethering to 26.3 ± 2.5 rolling cells per FOV (Fig. 6E). The rolling velocity on both selectins, 5.1 ± 1.3 μm/s, was similar to the rolling velocity on E-selectin/Fc alone (Fig. 6F).

To clearly illustrate the contribution of coimmobilized selectins, rolling flux quantities were calculated using equation (7) for low- and intermediate-density P-selectin, intermediate-density E-selectin, and coimmobilized E- and P-selectins (**Fig. 7A**) for the latest time-point in each group (~8 min after clamp

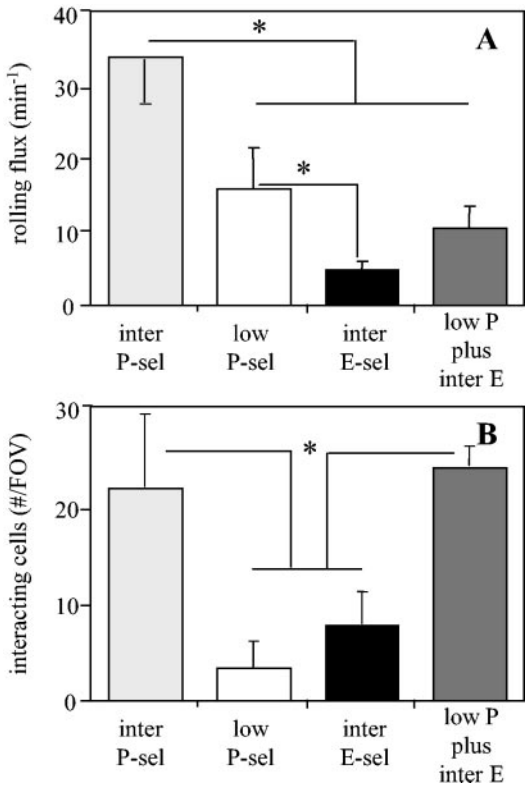


**Figure 7.** Flux (cells per minute; A) and numbers (B) of rolling GFP neutrophils per FOV on intermediate (150 ng/ml, light gray bars) or low-site density P-selectin/Fc (50 ng/ml, open bars), intermediate site-density E-selectin/Fc (150 ng/ml, solid bars), or coimmobilized P-selectin/Fc (50 ng/ml) and E-selectin/Fc (150 ng/ml, dark gray bars) 8 min after the initiation of autoperfusion. Each data point is mean ± SEM for at least four flow chambers from at least three different mice. *, Significant difference ($P<0.05$).

removal). Low- and intermediate-density P-selectin supports a significantly higher rolling flux (16±5 and 35±6.7 $min^{-1}$, respectively) than intermediate E-selectin (4.8±1.2 $min^{-1}$). Rolling flux on coimmobilized intermediate E- and low P-selectins was intermediate (10.6±3 $min^{-1}$), although not statistically different from low P-selectin alone. These data show that with coimmobilized selectins, P-selectin provides sufficient tethering capacity to allow a high number of rolling cells per FOV, and E-selectin is responsible for a low rolling velocity. These two effects lead to a dramatic increase in the number of rolling cells per FOV in the chambers where E- and P-selectins were coimmobilized compared with chambers with immobilized low P- or intermediate E-selectin alone (Fig. 7B). The rolling velocity on intermediate E-selectin (4.8±1.2 μm/s) was significantly lower than on low P-selectin (52±5 μm/s) but was similar to the rolling velocity on coimmobilized selectins (5.1±1.3 μm/s; Fig. 6, B, D, and F, respectively).

## DISCUSSION

This study introduces a novel, autoperfused micro-flow chamber system, which can be used to observe murine leukocyte rolling and adhesion in whole blood ex vivo. This is made possible by interconnecting a rectangular glass capillary to an autoperfused, extracorporal arterio-venous circuit. To measure wall shear stress, a pressure-transducer unit was integrated into the circuit. This approach requires no assumptions about the viscosity of blood, which is a complicated function of hematocrit, vessel size, and shear rate [47]. Two different tubing combinations were presented, allowing experimentation at low (~1.5 $dyn/cm^2$) or high (~10 $dyn/cm^2$) wall shear stress. The system is easy to set up and offers several advantages over already-existing and commercially available flow-chamber systems. Most prominently, this micro-flow chamber dramatically reduces the amount of cells necessary to conduct an experiment by decreasing the dead space and recirculating blood back into the mouse. There is no need for leukocyte isolation that may lead to considerable functional changes concerning the adhesive behavior of leukocytes [21–23].

Rheological evaluation of the system revealed stable flow conditions throughout the observation period with tolerable changes in blood-flow velocity and wall shear stress. Analysis of blood-flow velocity over time showed evidence of some pulsatility, which is present physiologically in arteries and veins [47]. The majority of the arterial-venous pressure drop in this system occurs in the PE10 or PE50 tubing. This tubing is typically 30–40 cm in length (15–20 cm for each of the jugular vein and carotid artery cannulas). With an ID of 0.28 or 0.58 mm and noting that resistance to flow is approximately proportional to diameter to the fourth power, it is not surprising that the vast majority of pressure drop occurs in the tubing, as the flow chamber is only 2–3 cm in length, and its hydraulic diameter is 0.36 mm.

Compared with conventional flow chambers, where cell suspensions are perfused through the chamber and then discarded, the autoperfused flow chamber system enables leukocytes and other blood constituents to recirculate. This may result in the release of activated leukocytes and proinflammatory cytokines into the systemic circulation. We did not note a change in systemic neutrophil or monocyte numbers throughout our experiments, which rules out significant pulmonary sequestration of leukocytes in the lungs (see Fig. 5). Also, flow chambers were used for no more than 10 min, and not more than four flow chambers were used per mouse. Although the majority of blood monocytes are $GFP^+$ (~65%) in the lys M-GFP mouse, it is likely that the majority of rolling $GFP^+$ leukocytes are neutrophils, which greatly outnumber monocytes in peripheral blood. In addition, a study by Reinhardt and Kubes [48] showed that P-selectin preferentially recruits neutrophils over monocytes, and E-selectin recruits each leukocyte subset equally well.

To functionally validate the flow chamber system for leukocyte rolling and adhesion studies, we performed experiments with P- and E-selectins immobilized on the inner surface of the glass capillary. The results show that GFP-expressing neutrophils interact with immobilized P- or E-selectin in a specific manner with rolling velocities comparable with in vivo measurements [27].

These data confirm that E-selectin is a poor tethering molecule, as has been suggested by intravital microscopy experiments in mice that lack P- and L-selectins [27, 28]. Leukocyte rolling flux and interaction density on E-selectin were significantly lower or similar, respectively, than on P-selectin coated at threefold-lower concentration (Fig. 7, A and B). In addition, increasing E-selectin-coating concentration fourfold only marginally increased the number of interacting cells per FOV, and this increase was only statistically significant at the latest time point (Fig. 6C). However, E-selectin mediates slow rolling even when coated at low concentrations, yielding site densities that are unable to support significant tethering. Although intermediate E-selectin/Fc supported a lower rolling flux than low P-selectin/Fc, the density of rolling cells per unit surface area was similar, caused by the lower rolling velocity [49–51]. Although we cannot exclude hydrodynamic or L-selectin-mediated secondary capture or tethering, we did not observe strings of cells typical of secondary capture [45, 46, 52]. Stroboscopic epi-illumination produces multiple images of the same cell in a field, creating the appearance of strings (Fig. 4), but this is an imaging artifact and not related to strings caused by secondary capture.

The most interesting finding of the present study is that P- and E-selectin have a synergistic effect on neutrophil accumulation. By coimmobilizing low-density P-selectin with intermediate-density E-selectin, rolling flux was similar to low P-selectin alone, but rolling velocity was similar to intermediate E-selectin alone, and interaction density was similar to intermediate P-selectin alone. This suggests that P-selectin tethers cells from free-flow, and E-selectin regulates rolling velocity. Together, E- and P-selectins synergize to dramatically increase the surface density of rolling cells. The number of interacting cells per FOV was dramatically increased on coimmobilized low P- and intermediate E-selectins above either selectin alone (Fig. 7B). Adding E-selectin reduces rolling velocity by >90% and enhances accumulation by more than sixfold compared with P-selectin alone. This increase was synergistic, as the number of interacting cells on coimmobilized selectins was more than twice the sum of E- and P-selectins immobilized

alone. Some synergistic effects were found when P-selectin was coimmobilized with ICAM-1 [37], but the effect was modest, reducing rolling velocity by only 30%. Although the overlapping function of E- and P-selectin has been known for almost a decade [31, 32], the present study is the first demonstration of a synergistic interaction.

## ACKNOWLEDGMENTS

National Institutes of Health HL54136 and EB02185 to K. L. supported this work. T32 GM 08715-01A1 to Gordon Laurie and K. L. supported M. L. S. M. L. S. and M. S. contributed equally to this work. We thank Michele Kirkpatrick for animal husbandry. Lys-GFP mice were a kind gift of Dr. T. Graf. We thank Dr. Brett Blackman (University of Virginia, Charlottesville) for useful discussions on fluid dynamics in the flow chamber.

## REFERENCES

1. Butcher, E. C. (1991) Leukocyte-endothelial cell recognition—three (or more) steps to specificity and diversity. *Cell* **67,** 1033–1036.
2. Smith, M. L., Long, D. S., Damiano, E. R., Ley, K. (2003) Near-wall μ-PIV reveals a hydrodynamically relevant endothelial surface layer in venules in vivo. *Biophys. J.* **85,** 637–645.
3. Mulivor, A. W., Lipowsky, H. H. (2002) Role of glycocalyx in leukocyte-endothelial cell adhesion. *Am. J. Physiol.* **283,** H1282–H1291.
4. Damiano, E. R., Westheider, J., Tözeren, A., Ley, K. (1996) Variation in the velocity, deformation, and adhesion energy density of leukocytes rolling within venules. *Circ. Res.* **79,** 1122–1130.
5. Jung, U., Ley, K. (1997) Regulation of E-selectin, P-selectin and ICAM-1 expression in mouse cremaster muscle vasculature. *Microcirculation* **4,** 311–319.
6. Lawrence, M. B., Springer, T. A. (1991) Leukocytes roll on a selectin at physiologic flow rates: Distinction from and prerequisite for adhesion through integrins. *Cell* **65,** 859–873.
7. Berlin, C., Bargatze, R. F., Campbell, J. J., von Andrian, U. H., Szabo, M. C., Hasslen, S. R., Nelson, R. D., Berg, E. L., Erlandsen, S. L., Butcher, E. C. (1995) $\alpha_4$ Integrins mediate lymphocyte attachment and rolling under physiologic flow. *Cell* **80,** 413–422.
8. Finger, E. B., Puri, K. D., Alon, R., Lawrence, M. B., von Andrian, U. H., Springer, T. A. (1996) Adhesion through L-selectin requires a threshold hydrodynamic shear. *Nature* **379,** 266–269.
9. Lawrence, M. B., Kansas, G. S., Ghosh, S., Kunkel, E. J., Ley, K. (1997) Threshold levels of fluid shear promote leukocyte adhesion through selectins (CD62L,P,E). *J. Cell Biol.* **136,** 717–727.
10. Rainger, G. E., Fisher, A. C., Nash, G. B. (1997) Endothelial-borne platelet-activating factor and interleukin-8 rapidly immobilize rolling neutrophils. *Am. J. Physiol.* **272,** H114–H122.
11. Campbell, J. J., Hedrick, J., Zlotnik, A., Siani, M. A., Thompson, D. A., Butcher, E. C. (1998) Chemokines and the arrest of lymphocytes rolling under flow conditions. *Science* **279,** 381–384.
12. Burrows, M. T. (1912) A method of furnishing a continuous supply of new medium to a tissue culture in vitro. *Anat. Rec.* **6,** 141–144.
13. Toy, B. L., Bardawil, W. A. (1958) A simple plastic perfusion chamber for continuous maintenance and cinematography of tissue cultures. *Exp. Cell Res.* **14,** 97–103.
14. Lawrence, M. B., McIntire, L. V., Eskin, S. G. (1987) Effect of flow on polymorphonuclear leukocyte/endothelial cell adhesion. *Blood* **70,** 1284–1290.
15. Usami, S., Chen, H. H., Zhao, Y., Chien, S., Skalak, R. (1993) Design and construction of a linear shear stress flow chamber. *Ann. Biomed. Eng.* **21,** 77–83.
16. Ruel, J., Lemay, J., Dumas, G., Doillon, C., Charara, J. (1995) Development of a parallel plate flow chamber for studying cell behavior under pulsatile flow. *ASAIO J.* **41,** 876–883.
17. Cao, J., Usami, S., Dong, C. (1997) Development of a side-view chamber for studying cell-surface adhesion under flow conditions. *Ann. Biomed. Eng.* **25,** 573–580.
18. Yuan, J., Melder, R. J., Jain, R. K., Munn, L. L. (2001) Lateral view flow system for studies of cell adhesion and deformation under flow conditions. *Biotechniques* **30,** 388–394.
19. Badimon, L., Turitto, V., Rosemark, J. A., Badimon, J. J., Fuster, V. (1987) Characterization of a tubular flow chamber for studying platelet interaction with biologic and prosthetic materials: deposition of indium 111-labeled platelets on collagen, subendothelium, and expanded polytetrafluoroethylene. *J. Lab. Clin. Med.* **110,** 706–718.
20. Abbitt, K. B., Nash, G. B. (2001) Characteristics of leucocyte adhesion directly observed in flowing whole blood in vitro. *Br. J. Haematol.* **112,** 55–63.
21. Glasser, L., Fiederlein, R. L. (1990) The effect of various cell separation procedures on assays of neutrophil function. A critical appraisal. *Am. J. Clin. Pathol.* **93,** 662–669.
22. Forsyth, K. D., Levinsky, R. J. (1990) Preparative procedures of cooling and re-warming increase leukocyte integrin expression and function on neutrophils. *J. Immunol. Methods* **128,** 159–163.
23. Kuijpers, T. W., Tool, A. T. J., van der Schoot, C. E., Ginsel, L. A., Onderwater, J. J. M., Roos, D., Verhoeven, A. J. (1991) Membrane surface antigen expression on neutrophils: a reappraisal of the use of surface markers for neutrophil activation. *Blood* **78,** 1105–1111.
24. Brown, D. C., Larson, R. S. (2001) Improvements to parallel plate flow chambers to reduce reagent and cellular requirements. *BMC Immunol.* **2,** 9.
25. Cotter, M. J., Norman, K. E., Hellewell, P. G., Ridger, V. C. (2001) A novel method for isolation of neutrophils from murine blood using negative immunomagnetic separation. *Am. J. Pathol.* **159,** 473–481.
26. Faust, N., Varas, F., Kelly, L. M., Heck, S., Graf, T. (2000) Insertion of enhanced green fluorescent protein into the lysozyme gene creates mice with green fluorescent granulocytes and macrophages. *Blood* **96,** 719–726.
27. Jung, U., Ley, K. (1999) Mice lacking two or all three selectins demonstrate overlapping and distinct functions of each selectin. *J. Immunol.* **162,** 6755–6762.
28. Robinson, S. D., Frenette, P. S., Rayburn, H., Cummiskey, M., Ullman-Cullere, M., Wagner, D. D., Hynes, R. O. (1999) Multiple, targeted deficiencies in selectins reveal a predominant role for P-selectin in leukocyte recruitment. *Proc. Natl. Acad. Sci. USA* **96,** 11452–11457.
29. Kunkel, E. J., Ley, K. (1996) Distinct phenotype of E-selectin deficient mice: E-selectin is required for slow leukocyte rolling in vivo. *Circ. Res.* **79,** 1196–1204.
30. Smith, M. J., Berg, E. L., Lawrence, M. B. (1999) A direct comparison of selectin-mediated transient adhesive events using high temporal resolution. *Biophys. J.* **77,** 3371–3383.
31. Bullard, D. C., Kunkel, E. J., Kubo, H., Hicks, M. J., Lorenzo, I., Doyle, N. A., Doerschuk, C. M., Ley, K., Beaudet, A. L. (1996) Infectious susceptibility and severe deficiency of leukocyte rolling and recruitment in E-selectin and P-selectin double mutant mice. *J. Exp. Med.* **183,** 2329–2336.
32. Frenette, P. S., Mayadas, T. N., Rayburn, H., Hynes, R. O., Wagner, D. D. (1996) Susceptibility to infection and altered hematopoiesis in mice deficient in both P- and E-selectins. *Cell* **84,** 563–574.
33. Ellies, L. G., Tsuboi, S., Petryniak, B., Lowe, J. B., Fukuda, M., Marth, J. D. (1998) Core 2 oligosaccharide biosynthesis distinguishes between selectin ligands essential for leukocyte homing and inflammation. *Immunity* **9,** 881–890.
34. Bosse, R., Vestweber, D. (1994) Only simultaneous blocking of the L- and P-selectin completely inhibits neutrophil migration into mouse peritoneum. *Eur. J. Immunol.* **24,** 3019–3024.
35. Norton, C. R., Rumberger, J. M., Burns, D. K., Wolitzky, B. A. (1993) Characterization of murine E-selectin expression in vitro using novel anti-mouse E-selectin monoclonal antibodies. *Biochem. Biophys. Res. Commun.* **195,** 250–258.
36. Lagasse, E., Weissman, I. L. (1996) Flow cytometric identification of murine neutrophils and monocytes. *J. Immunol. Methods* **197,** 139–150.
37. DiVietro, J. A., Smith, M. J., Smith, B. R., Petruzzelli, L., Larson, R. S., Lawrence, M. B. (2001) Immobilized IL-8 triggers progressive activation of neutrophils rolling in vitro on P-selectin and intercellular adhesion molecule-1. *J. Immunol.* **167,** 4017–4025.
38. Zhang, Y., Neelamegham, S. (2002) Estimating the efficiency of cell capture and arrest in flow chambers: study of neutrophil binding via E-selectin and ICAM-1. *Biophys. J.* **83,** 1934–1952.
39. White, F. M. (2003) Viscous flow in ducts. In *Fluid Mechanics*, Columbus, OH, McGraw Hill, 343–450.
40. White, F. M. (2003) Flow past immersed bodies. In *Fluid Mechanics*, Columbus, OH, McGraw Hill,. 451–522.
41. Cokelet, G. R. (1999) Viscometric, in vitro and in vivo blood viscosity relationships: how are they related? *Biorheology* **36,** 343–358.

42. Loudon, C., Tordesillas, A. (1998) The use of the dimensionless Womersley number to characterize the unsteady nature of internal flow. *J. Theor. Biol.* **191,** 63–78.
43. Ku, D. N. (1997) Blood flow in arteries. *Annu. Rev. Fluid Mech.* **29,** 399–434.
44. Norman, K. E. (2001) An effective and economical solution for digitizing and analyzing video recordings in the microcirculation. *Microcirculation* **8,** 243–249.
45. King, M. R., Hammer, D. A. (2001) Multiparticle adhesive dynamics: hydrodynamic recruitment of rolling leukocytes. *Proc. Natl. Acad. Sci. USA* **98,** 14919–14924.
46. St Hill, C. A., Alexander, S. R., Walcheck, B. (2003) Indirect capture augments leukocyte accumulation on P-selectin in flowing whole blood. *J. Leukoc.Biol.* **73,** 464–471.
47. Chien, S., Usami, S., Skalak, R. (1984) Blood flow in small tubes. In *Handbook of Physiology* (E. M. Renkin and C. C. Michel, eds.), Bethesda, MD, American Physiological Society, 217–249.
48. Reinhardt, P. H., Kubes, P. (1998) Differential leukocyte recruitment from whole blood via endothelial adhesion molecules under shear conditions. *Blood* **92,** 4691–4699.
49. Ley, K., Gaehtgens, P. (1991) Endothelial, not hemodynamic, differences are responsible for preferential leukocyte rolling in venules. *Circ. Res.* **69,** 1034–1041.
50. Jung, U., Norman, K. E., Ramos, C. L., Scharffetter-Kochanek, K., Beaudet, A. L., Ley, K. (1998) Transit time of leukocytes rolling through venules controls cytokine-induced inflammatory cell recruitment in vivo. *J. Clin. Invest.* **102,** 1526–1533.
51. Fiebig, E., Ley, K., Arfors, K-E. (1991) Rapid leukocyte accumulation by "spontaneous" rolling and adhesion in the exteriorized rabbit mesentery. *Int. J. Microcirc. Clin. Exper.* **10,** 127–144.
52. King, M. R., Kim, M. B., Sarelius, I. H., Hammer, D. A. (2003) Hydrodynamic interactions between rolling leukocytes in vivo. *Microcirculation* **10,** 401–409.